

# Optimal Hedge Ratio for Delta-Neutral Liquidity Provision under Liquidation Constraints

Atsushi Hane\*

March 2026

## Abstract

We study the problem of optimally hedging the price exposure of liquidity positions in constant-product automated market makers (AMMs) when the hedge is funded by collateralized borrowing. A liquidity provider (LP) who borrows tokens to construct a delta-neutral position faces a trade-off: higher hedge ratios reduce price exposure but increase liquidation risk through tighter collateral utilization. We model token prices as correlated geometric Brownian motions and derive the hedge ratio  $h$  that maximizes risk-adjusted return subject to a liquidation-probability constraint expressed via a first-passage-time bound. The unconstrained optimum  $h^*$  admits a closed-form expression, but at  $h^*$  the liquidation probability is prohibitively high. The practical optimum  $h^{**} = \min(h^*, \bar{h}(\alpha))$  is determined by the binding liquidation constraint  $\bar{h}(\alpha)$ , which we evaluate analytically via the first-passage-time formula and confirm with Monte Carlo simulation. Simulations calibrated to on-chain data validate the analytical results, demonstrate robustness across realistic parameter ranges, and show that the optimal hedge ratio lies between 50% and 70% for typical DeFi lending conditions. Practical guidelines for rebalancing frequency and position sizing are also provided.

**Keywords:** decentralized finance, liquidity provision, impermanent loss, delta hedging, liquidation risk, first passage time

**JEL Classification:** G11, G23, C63

## 1 Introduction

Automated market makers (AMMs) such as Uniswap v2 [Adams et al., 2020] have become a cornerstone of decentralized finance (DeFi; see Xu et al. 2023 for a comprehensive survey), enabling permissionless token exchange via constant-product liquidity pools. Liquidity providers earn trading fees but are exposed to *impermanent loss* (IL)—the shortfall relative to a simple buy-and-hold portfolio when token prices diverge.<sup>1</sup>

---

\*Independent researcher. Email: [atsushihane@gmail.com](mailto:atsushihane@gmail.com)

<sup>1</sup>Milionis et al. [2022] argue that the relevant LP cost metric is *fees - LVR* rather than IL. Our framework hedges pure price exposure, not non-linear costs such as IL or LVR; see Remark 3.

A natural mitigation is to *borrow* the constituent tokens from a lending protocol and sell them, creating a short position that offsets the LP’s long exposure. This “delta-neutral” approach is widely discussed in practitioner forums, yet a rigorous treatment of the resulting *liquidation risk* is absent from the literature.

The contribution of this paper is threefold:

1. We formalize the LP hedging problem as a stochastic optimization over the hedge ratio  $h$ , incorporating borrowing costs, reward income, and a hard loan-to-value (LTV) constraint.
2. We derive the unconstrained optimal hedge ratio  $h^*$  in closed form and show that the practical optimum  $h^{**}$  is determined by the binding liquidation constraint, whose threshold  $\bar{h}(\alpha)$  is characterized via a first-passage-time approximation.
3. We validate the model with Monte Carlo simulation calibrated to on-chain pool and lending data, and provide actionable rebalancing rules.

The remainder of the paper is organized as follows. Section 2 reviews related work. Section 3 presents the model. Section 4 derives the optimal hedge ratio. Section 5 analyzes liquidation probability using first-passage-time theory. Section 6 describes the Monte Carlo study. Section 7 reports the results. Section 8 discusses practical implications. Section 9 concludes.

## 2 Related Work

**Impermanent loss.** The concept of IL in constant-product AMMs was first described informally by Pintail [2019] and formalized in the Uniswap v2 whitepaper [Adams et al., 2020]. Aigner and Dhaliwal [2021] quantified IL under geometric Brownian motion and derived closed-form expressions for expected IL as a function of volatility. Clark [2020] provided a similar analysis with emphasis on replication strategies. Loesch et al. [2021] extended the analysis to concentrated-liquidity AMMs (Uniswap v3). Angeris et al. [2020] established rigorous theoretical foundations for constant-product markets, proving that AMM prices must closely track external market prices under no-arbitrage conditions. Milionis et al. [2022] introduce *loss-versus-rebalancing* (LVR), a distinct, path-dependent measure of the adverse-selection cost that LPs bear by offering a continuous trading option to arbitrageurs; while related to IL, LVR is monotonically increasing and captures costs that IL—being path-independent—does not. Evans et al. [2022] derive optimal fee structures to compensate LPs for adverse selection, while Heimbach et al. [2022] provide empirical evidence that maximal-extractable-value (MEV) activity amplifies LP losses beyond what IL alone predicts.

**Delta-neutral strategies.** Khakhar and Chen [2022] propose a delta-hedging algorithm for LP positions using options on the underlying tokens, but do not derive an optimal hedge ratio or model liquidation risk from the hedging instrument itself. Lipton et al. [2025] develop a unified framework for hedging LP price exposure via static option replication and dynamic delta-hedging, covering both Uniswap v2 and v3; their approach assumes access to liquid options markets, which remain largely unavailable in DeFi. Capponi and Jia [2021] study optimal portfolio allocation in decentralized exchanges, and Fan et al. [2022] analyze differential liquidity provision in concentrated-liquidity AMMs. To

the best of our knowledge, no prior work explicitly models the hedge ratio as a continuous decision variable subject to a liquidation constraint arising from collateralized borrowing.

**Liquidation risk in DeFi lending.** Qin et al. [2022] and Perez et al. [2021] study liquidation cascades in lending protocols from a systemic-risk perspective. Gudgeon et al. [2020] analyze the design of DeFi lending protocols and the role of liquidation mechanisms. Bartoletti et al. [2021] provide a systematic classification of DeFi protocols and their composability risks, including cascading liquidations across lending and AMM layers. Our work differs by focusing on the *individual* LP’s problem of choosing a hedge ratio that balances variance reduction against liquidation probability.

**First passage time.** The first-passage-time theory for Brownian motion is classical [Karatzas and Shreve, 1991]. We apply it to the LTV process via a moment-matching approximation for the sum of correlated geometric Brownian motions, following the approach of Milevsky [1998].

## 3 Model

### 3.1 Price dynamics

Let  $S_t^A$  and  $S_t^B$  denote the prices of tokens  $A$  and  $B$  at time  $t$ , measured in a numéraire (e.g., USDC). We model prices as correlated geometric Brownian motions:

$$\frac{dS_t^A}{S_t^A} = \mu_A dt + \sigma_A dW_t^A, \quad (1)$$

$$\frac{dS_t^B}{S_t^B} = \mu_B dt + \sigma_B dW_t^B, \quad (2)$$

where  $dW_t^A dW_t^B = \rho dt$  and  $\rho \in (-1, 1)$  is the instantaneous correlation.

### 3.2 Constant-product AMM

A constant-product pool maintains the invariant  $x_t \cdot y_t = L^2$ , where  $x_t$  and  $y_t$  are the reserves of tokens  $A$  and  $B$ , and  $L$  is the liquidity parameter. An LP who deposits value  $V_0$  at time 0 holds a claim whose *mark-to-market value* (excluding accumulated trading fees and farming rewards) at time  $t$  is

$$V_t^{\text{LP}} = V_0 \sqrt{\frac{S_t^A}{S_0^A} \cdot \frac{S_t^B}{S_0^B}}. \quad (3)$$

Fee and reward income is accounted for separately via the cumulative reward term  $R_t$  in (5).

### 3.3 Hedging via borrowing

The LP deposits collateral  $C$  (in stablecoin) into a lending protocol and borrows fractions of tokens  $A$  and  $B$ . Define the *hedge ratio*  $h \in [0, 1]$  as the fraction of LP token exposure

that is offset by the borrowed position. At inception the LP borrows

$$D_0^A = h \cdot \frac{V_0}{2S_0^A}, \quad D_0^B = h \cdot \frac{V_0}{2S_0^B} \quad (4)$$

tokens  $A$  and  $B$ , and uses them, together with spot-purchased tokens, to fund the LP position. The borrow rates are  $r_A$  and  $r_B$  per annum.

### 3.4 Portfolio value

The LP funds the position with a mix of equity and borrowed tokens. Equity capital deployed is  $C + (1-h)V_0$ : the collateral  $C$  (in stablecoin, deposited in the lending protocol) plus  $(1-h)V_0$  used to purchase the unhedged fraction of LP tokens. The borrowed tokens go directly into the LP alongside the spot-purchased ones.

The net portfolio value at time  $t$  (before rebalancing) is

$$\Pi_t = \underbrace{V_t^{\text{LP}} + R_t}_{\text{LP + rewards}} + \underbrace{C(1+r_f t)}_{\text{collateral + yield}} - \underbrace{\frac{hV_0}{2} \left( \frac{S_t^A}{S_0^A} + \frac{S_t^B}{S_0^B} \right)}_{\text{debt value}} - \underbrace{\frac{hV_0}{2}(r_A + r_B)t}_{\text{borrow cost}} \quad (5)$$

where  $R_t$  denotes cumulative LP rewards (fees + incentives), growing linearly as  $R_t = (R/V_0)V_0 t$  with  $R/V_0$  the annualized reward-to-value ratio (Table 2), and  $r_f$  is the stablecoin supply rate earned on collateral.

### 3.5 Loan-to-value constraint

The lending protocol liquidates the position if the loan-to-value ratio exceeds a threshold  $\ell_{\max}$ :

$$\text{LTV}_t = \frac{\frac{hV_0}{2} \left( \frac{S_t^A}{S_0^A} + \frac{S_t^B}{S_0^B} \right)}{C} \leq \ell_{\max}. \quad (6)$$

The numerator (debt in USD) grows when token prices rise, while the denominator (stablecoin collateral) is fixed. Note that  $\text{LTV}_0 = hV_0/C$ , so higher hedge ratios start with higher leverage.

**Remark 1** (Accrued interest). *Equation (6) omits accrued borrow interest from the numerator. Including it would add a term  $\frac{hV_0}{2}(r_A + r_B)t$  to the debt, raising LTV by  $\frac{hV_0(r_A+r_B)t}{2C}$ . At the calibrated values ( $h = 0.60$ ,  $r_A + r_B = 0.18$ ,  $T = 0.25$ ,  $C/V_0 = 2.0$ ), this amounts to  $\approx 0.7$  pp of LTV—negligible relative to the 50 pp buffer between initial LTV (30%) and  $\ell_{\max}$  (80%). The Monte Carlo simulation (Section 6) does incorporate accrued interest in the daily LTV check, so all numerical results account for this effect; only the analytical expressions in Sections 4 and 5 use the simplified form (6).*

## 4 Optimal Hedge Ratio

Throughout this section we set  $\mu_A = \mu_B = 0$  in (1)–(2). This is *not* an appeal to risk-neutral pricing (no derivative is being priced); rather, it reflects the assumption that the LP holds no directional view on token prices and regards reward income as the sole source of expected profit. The zero-drift assumption is analytically convenient and conservative in bull markets: any positive drift in token prices would increase debt value and thus

worsen liquidation risk, making our estimates an upper bound on feasible hedge ratios. Conversely, in bear markets ( $\mu < 0$ ), falling prices reduce debt value and improve LTV, so the short leg generates profit and the liquidation constraint relaxes. The optimal  $h^{**}$  would then increase, meaning the zero-drift estimates are conservative in both directions: they understate the feasible hedge ratio in bear markets and overstate it in bull markets.

## 4.1 Objective function

We adopt the Sharpe ratio as the objective for analytical tractability and comparability with the traditional hedging literature. While the return distribution exhibits a mass point at the liquidation loss (visible in Table 3 as the discontinuous VaR jump between  $h = 0.70$  and  $h = 0.80$ ), the 5% VaR reported alongside confirms that the Sharpe-optimal  $h^{**}$  also performs well under tail-risk criteria. A formal CVaR optimization is left for future work.

We maximize the Sharpe ratio of the dollar profit and loss  $\Pi_T - \Pi_0$  over the hedge ratio  $h$ :

$$h^* = \arg \max_{h \in [0,1]} \frac{\mathbb{E}[\Pi_T - \Pi_0]}{\sqrt{\text{Var}(\Pi_T)}} \quad \text{s.t.} \quad \Pr(\exists t \in [0, T] : \text{LTV}_t > \ell_{\max}) \leq \alpha. \quad (7)$$

We first solve the unconstrained problem (ignoring the liquidation constraint) and then incorporate the constraint in Section 5.

**Remark 2** (Dollar vs. ROE-based Sharpe ratio). *The analytical derivation maximizes the Sharpe ratio of dollar P&L  $\Pi_T - \Pi_0$ . The Monte Carlo analysis (Section 6) instead reports the Sharpe ratio of ROE :=  $(\Pi_T - \Pi_0)/\Pi_0$ , where  $\Pi_0 = C + (1 - h)V_0$  (Eq. 9). Since  $\Pi_0$  depends on  $h$ , the two objectives are not identical. However, for  $C/V_0 = 2.0$  the equity base varies by at most a factor of  $3.0/2.0 = 1.5$  across  $h \in [0, 1]$ , and both criteria agree on the location of  $h^{**}$  because the practical optimum is determined by the binding liquidation constraint (Remark 5), not by the unconstrained FOC.*

## 4.2 Lognormal moment lemma

The following identity is used repeatedly.

**Lemma 1.** *Let  $X_T = \ln(S_T^A/S_0^A)$  and  $Y_T = \ln(S_T^B/S_0^B)$ . Under zero-drift GBM ( $\mu_A = \mu_B = 0$ ), the joint moment generating function is*

$$\mathbb{E}[e^{aX_T + bY_T}] = \exp\left(\frac{a(a-1)\sigma_A^2 + b(b-1)\sigma_B^2 + 2ab\rho\sigma_A\sigma_B}{2} T\right) \quad (8)$$

for all  $a, b \in \mathbb{R}$ .

*Proof.* Under zero-drift GBM,  $X_T \sim \mathcal{N}(-\frac{1}{2}\sigma_A^2 T, \sigma_A^2 T)$  and  $Y_T \sim \mathcal{N}(-\frac{1}{2}\sigma_B^2 T, \sigma_B^2 T)$  with  $\text{Cov}(X_T, Y_T) = \rho\sigma_A\sigma_B T$ . The linear combination  $aX_T + bY_T$  is normal with mean  $-(a\sigma_A^2 + b\sigma_B^2)T/2$  and variance  $(a^2\sigma_A^2 + b^2\sigma_B^2 + 2ab\rho\sigma_A\sigma_B)T$ . Applying the lognormal MGF  $\mathbb{E}[e^Z] = e^{\mu_Z + \sigma_Z^2/2}$  and simplifying yields (8).  $\square$

Table 1 collects the moments used below, each obtained by substituting the appropriate  $(a, b)$  into Lemma 1.

Table 1: Key lognormal moments under zero-drift GBM ( $\mu_A = \mu_B = 0$ ,  $p_i := S_T^i/S_0^i$ ).

Quantity	$(a, b)$	Expression
$\mathbb{E}[p_A]$	$(1, 0)$	1
$\mathbb{E}[p_B]$	$(0, 1)$	1
$\mathbb{E}[\sqrt{p_A p_B}]$	$(\frac{1}{2}, \frac{1}{2})$	$e^{-\phi T}$ , $\phi := \frac{\sigma_A^2 + \sigma_B^2 - 2\rho\sigma_A\sigma_B}{8}$
$\mathbb{E}[p_A p_B]$	$(1, 1)$	$e^{\rho\sigma_A\sigma_B T}$
$\mathbb{E}[p_A^2]$	$(2, 0)$	$e^{\sigma_A^2 T}$
$\mathbb{E}[p_B^2]$	$(0, 2)$	$e^{\sigma_B^2 T}$
$\mathbb{E}[p_A^{3/2} p_B^{1/2}]$	$(\frac{3}{2}, \frac{1}{2})$	$e^{(3\sigma_A^2 - \sigma_B^2 + 6\rho\sigma_A\sigma_B) T/8}$
$\mathbb{E}[p_A^{1/2} p_B^{3/2}]$	$(\frac{1}{2}, \frac{3}{2})$	$e^{(-\sigma_A^2 + 3\sigma_B^2 + 6\rho\sigma_A\sigma_B) T/8}$

### 4.3 Expected return

Write  $p_i = S_T^i/S_0^i$  for the price relatives. The initial equity is

$$\Pi_0 = C + (1 - h)V_0, \quad (9)$$

since the LP deposits  $C$  as collateral and spends  $(1 - h)V_0$  to purchase the unhedged fraction of LP tokens. From (5) the P&L is

$$\Pi_T - \Pi_0 = \underbrace{V_0(\sqrt{p_A p_B} - 1)}_{\Delta V^{\text{LP}}} + RT + Cr_f T - \frac{hV_0}{2}(p_A + p_B - 2) - \frac{hV_0}{2}(r_A + r_B)T, \quad (10)$$

where  $R$  is the reward rate in dollars per year (so that  $RT$  is total reward income over the horizon) and  $r_f$  is the stablecoin supply rate (per annum). In Table 2,  $R/V_0 = 0.54$  means annual reward income equals 54% of LP value.

**Proposition 2** (Expected P&L). *Under zero-drift GBM,*

$$\mathbb{E}[\Pi_T - \Pi_0] = V_0(e^{-\phi T} - 1) + RT + Cr_f T - \frac{hV_0}{2}(r_A + r_B)T, \quad (11)$$

where  $\phi = (\sigma_A^2 + \sigma_B^2 - 2\rho\sigma_A\sigma_B)/8$  governs the expected rate of LP value decay due to price divergence.

*Proof.* Apply  $\mathbb{E}[p_A] = \mathbb{E}[p_B] = 1$  (Table 1) to (10). The hedge-related price term  $\mathbb{E}[\frac{hV_0}{2}(p_A + p_B - 2)] = 0$  vanishes, leaving only the deterministic borrow cost  $\frac{hV_0}{2}(r_A + r_B)T$ .  $\square$

**Remark 3.** *The expected LP value change  $V_0(e^{-\phi T} - 1)$ —the structural cost of price divergence, commonly called impermanent loss—is independent of  $h$ . The hedge ratio affects expected return only through borrow costs, which are linear in  $h$ . The benefit of hedging is entirely through variance reduction: the borrowing-based hedge targets price exposure, not the non-linear divergence cost itself.*

## 4.4 Variance of return

The only stochastic terms in (10) are  $G := \sqrt{p_A p_B}$  (the LP value factor) and  $A := \frac{1}{2}(p_A + p_B)$  (the arithmetic mean of price relatives).

**Proposition 3** (Variance decomposition).

$$\text{Var}(\Pi_T) = V_0^2 [v_{GG} + h^2 v_{AA} - 2h v_{GA}], \quad (12)$$

where

$$v_{GG} := \text{Var}(G) = e^{\rho\sigma_A\sigma_B T} - e^{-2\phi T}, \quad (13)$$

$$v_{AA} := \text{Var}(A) = \frac{1}{4} [e^{\sigma_A^2 T} + e^{\sigma_B^2 T} + 2e^{\rho\sigma_A\sigma_B T} - 4], \quad (14)$$

$$v_{GA} := \text{Cov}(G, A) = \frac{1}{2} [e^{(3\sigma_A^2 - \sigma_B^2 + 6\rho\sigma_A\sigma_B)T/8} + e^{(-\sigma_A^2 + 3\sigma_B^2 + 6\rho\sigma_A\sigma_B)T/8} - 2e^{-\phi T}]. \quad (15)$$

*Proof.* From (10),  $\text{Var}(\Pi_T) = V_0^2 \text{Var}(G - hA) = V_0^2 [\text{Var}(G) + h^2 \text{Var}(A) - 2h \text{Cov}(G, A)]$ .

For  $v_{GG}$ :  $\text{Var}(G) = \mathbb{E}[G^2] - (\mathbb{E}[G])^2 = e^{\rho\sigma_A\sigma_B T} - e^{-2\phi T}$  using Table 1 with  $(a, b) = (1, 1)$  and  $(\frac{1}{2}, \frac{1}{2})$ .

For  $v_{AA}$ :  $\text{Var}(A) = \frac{1}{4} [\text{Var}(p_A) + \text{Var}(p_B) + 2\text{Cov}(p_A, p_B)]$  with  $\text{Var}(p_i) = \mathbb{E}[p_i^2] - 1$  and  $\text{Cov}(p_A, p_B) = \mathbb{E}[p_A p_B] - 1$ .

For  $v_{GA}$ :  $\text{Cov}(G, A) = \frac{1}{2} [\mathbb{E}[G p_A] + \mathbb{E}[G p_B]] - \mathbb{E}[G]$  where  $\mathbb{E}[G p_A] = \mathbb{E}[p_A^{3/2} p_B^{1/2}]$  and  $\mathbb{E}[G p_B] = \mathbb{E}[p_A^{1/2} p_B^{3/2}]$  from Table 1.  $\square$

**Remark 4.** The variance (12) is a convex quadratic in  $h$  with minimum at the minimum-variance hedge ratio  $h_{\text{mv}} = v_{GA}/v_{AA}$ . Under the calibration in Table 2,  $h_{\text{mv}} \approx 0.977$ .

## 4.5 Unconstrained optimal hedge ratio

Define the expected excess P&L and its derivative:

$$\mu(h) := \mathbb{E}[\Pi_T - \Pi_0] = \mu_0 - c h, \quad (16)$$

$$c := \frac{V_0}{2} (r_A + r_B) T > 0, \quad (17)$$

where  $\mu_0 := V_0(e^{-\phi T} - 1) + RT + Cr_f T$  collects the  $h$ -independent terms. Since  $c > 0$ , expected return decreases linearly in  $h$ .

The Sharpe ratio is

$$\text{SR}(h) = \frac{\mu_0 - c h}{V_0 \sqrt{v_{GG} + h^2 v_{AA} - 2h v_{GA}}}. \quad (18)$$

**Theorem 4** (Optimal hedge ratio). Assume  $\mu_0 > 0$  (the strategy is profitable at  $h = 0$ ) and  $c > 0$  (borrowing is costly). The unconstrained maximizer of  $\text{SR}(h)$  satisfies the linear first-order condition

$$h(\mu_0 v_{AA} - c v_{GA}) = \mu_0 v_{GA} - c v_{GG}, \quad (19)$$

with unique solution

$$h^* = \frac{\mu_0 v_{GA} - c v_{GG}}{\mu_0 v_{AA} - c v_{GA}}. \quad (20)$$

When borrowing is free ( $c = 0$ ), this reduces to the minimum-variance hedge ratio  $h_{\text{mv}} = v_{GA}/v_{AA}$ .

*Proof.* Setting  $dSR/dh = 0$  and clearing denominators yields the condition

$$\mu'(h) \sigma^2(h) = \mu(h) \frac{1}{2} \frac{d\sigma^2}{dh}(h), \quad (21)$$

where  $\sigma^2(h) = V_0^2(v_{GG} + h^2v_{AA} - 2hv_{GA})$ . Substituting  $\mu'(h) = -c$  and  $d\sigma^2/dh = V_0^2(2hv_{AA} - 2v_{GA})$ :

$$-c(v_{GG} + h^2v_{AA} - 2hv_{GA}) = (\mu_0 - ch)(hv_{AA} - v_{GA}).$$

Expanding both sides, the  $ch^2v_{AA}$  terms cancel, leaving the linear equation (19). The second-order condition  $SR''(h^*) < 0$  is verified in Appendix B.  $\square$

**Corollary 5** (Near-full unconstrained hedge). *When  $c/\mu_0 \ll 1$  (reward rates dominate borrow costs),  $h^* \approx h_{mv} = v_{GA}/v_{AA}$ . For token pairs with similar volatilities ( $\sigma_A \approx \sigma_B$ ) and moderately positive correlation,  $h_{mv}$  is close to 1, so the unconstrained optimum calls for nearly complete hedging.*

*Proof.* From (20), as  $c \rightarrow 0$ ,  $h^* \rightarrow v_{GA}/v_{AA} = h_{mv}$ . Since  $v_{GA} \leq \sqrt{v_{GG}v_{AA}}$  by Cauchy-Schwarz,  $h_{mv} \leq \sqrt{v_{GG}/v_{AA}}$ . When  $\sigma_A \approx \sigma_B$ ,  $v_{GG} \approx v_{AA}$ , so  $h_{mv} \approx 1$ .  $\square$

**Remark 5.** *This is the paper's central result. Under the calibration in Table 2,  $h^* = 0.977$  (Theorem 4), meaning the unconstrained optimum is near-full hedging. However, at  $h = 0.977$  the liquidation probability exceeds 19% (Table 4), far above any reasonable tolerance. The liquidation constraint forces the feasible hedge ratio down to  $h^{**} \approx 0.60$ – $0.65$ , where liquidation probability drops to 1.4–2.3%. Thus the practical interior optimum arises not from the Sharpe maximization itself, but from the binding liquidation constraint, as formalized in Section 5.*

## 4.6 Numerical illustration

Using the calibration in Table 2 ( $\sigma_A = 0.922$ ,  $\sigma_B = 1.084$ ,  $\rho = 0.72$ ,  $r_A = 0.03$ ,  $r_B = 0.15$ ,  $R/V_0 = 0.54$ ,  $C/V_0 = 2.0$ ,  $T = 0.25$ ), we compute:

$$\begin{aligned} \phi &= 0.0732, & v_{GG} &= 0.2331, & v_{AA} &= 0.2431, & v_{GA} &= 0.2376, \\ \mu_0/V_0 &= 0.1369, & c/V_0 &= 0.0225, & h_{mv} &= 0.977. \end{aligned}$$

The unconstrained solution (20) gives  $h^* = 0.977 \approx 1$ , confirming that the optimal unconstrained hedge is nearly complete (Corollary 5). The analytical Sharpe ratio rises steeply as  $h \rightarrow h^*$ :

$h$	0.0	0.3	0.5	0.6	0.7	0.8	$h^*$	1.0
SR( $h$ )	0.28	0.39	0.53	0.65	0.87	1.29	3.88	3.62

However, the Monte Carlo simulation (which incorporates liquidation losses as a 20% collateral penalty) yields an effective Sharpe peak at  $h = 0.60$ . At  $h^* = 0.977$  the liquidation probability exceeds 19%, destroying risk-adjusted returns. This confirms that the *liquidation constraint is the binding factor* that forces  $h^{**}$  well below  $h^*$  (Remark 5).

## 5 Liquidation Probability via First Passage Time

The liquidation constraint in (7) requires bounding the probability that the LTV process exceeds  $\ell_{\max}$  at any point during the horizon  $[0, T]$ . This is a first-passage-time problem.

### 5.1 LTV dynamics

From (6), the LTV at time  $t$  is

$$\text{LTV}_t = \frac{hV_0}{2C} \left( \frac{S_t^A}{S_0^A} + \frac{S_t^B}{S_0^B} \right) = \frac{hV_0}{2C} (p_A(t) + p_B(t)), \quad (22)$$

where  $p_i(t) = S_t^i/S_0^i$  are GBM processes. The initial value is  $\text{LTV}_0 = hV_0/C$ .

The process  $Z_t := p_A(t) + p_B(t)$  is the sum of two correlated geometric Brownian motions. Exact first-passage-time distributions for sums of GBMs are not available in closed form, so we employ a moment-matching approximation.

### 5.2 Moment-matched GBM approximation

We approximate  $Z_t$  by a single GBM  $\hat{Z}_t$  with the same first two moments. Under zero-drift dynamics:

$$\mathbb{E}[Z_t] = 2, \quad (23)$$

$$\mathbb{E}[Z_t^2] = e^{\sigma_A^2 t} + e^{\sigma_B^2 t} + 2e^{\rho\sigma_A\sigma_B t}. \quad (24)$$

Matching  $\hat{Z}_t = 2 \exp((\tilde{\mu} - \tilde{\sigma}^2/2)t + \tilde{\sigma}\tilde{W}_t)$  to these moments gives the approximation parameters:

$$\tilde{\mu} = 0, \quad (25)$$

$$\tilde{\sigma}^2 = \frac{1}{t} \ln \left( \frac{e^{\sigma_A^2 t} + e^{\sigma_B^2 t} + 2e^{\rho\sigma_A\sigma_B t}}{4} \right). \quad (26)$$

For small  $t$ ,  $\tilde{\sigma}^2 \approx (\sigma_A^2 + \sigma_B^2 + 2\rho\sigma_A\sigma_B)/4$ , which is the variance of the equally-weighted portfolio.

### 5.3 First passage time to liquidation

Define the first passage time  $\tau = \inf\{t \geq 0 : \text{LTV}_t \geq \ell_{\max}\}$ . Under the GBM approximation,  $\text{LTV}_t/\text{LTV}_0 \approx \hat{Z}_t/2$ , and the liquidation boundary in log-space is  $b = \ln(\ell_{\max}/\text{LTV}_0)$ .

**Proposition 6** (Approximate liquidation probability). *Under the moment-matched GBM approximation with drift  $\tilde{\mu} = 0$  and volatility  $\tilde{\sigma}$ , define the log-process drift  $\nu := \tilde{\mu} - \tilde{\sigma}^2/2 = -\tilde{\sigma}^2/2$ . The probability of liquidation during  $[0, T]$  is*

$$\Pr(\tau \leq T) \approx \Phi \left( \frac{-b - \frac{\tilde{\sigma}^2}{2} T}{\tilde{\sigma}\sqrt{T}} \right) + \frac{\text{LTV}_0}{\ell_{\max}} \Phi \left( \frac{-b + \frac{\tilde{\sigma}^2}{2} T}{\tilde{\sigma}\sqrt{T}} \right), \quad (27)$$

where  $b = \ln(\ell_{\max}C/(hV_0)) = \ln(\ell_{\max}/\text{LTV}_0)$  is the log-distance to the liquidation barrier,  $\Phi$  is the standard normal CDF, and the coefficient  $e^{2\nu b/\tilde{\sigma}^2} = e^{-b} = \text{LTV}_0/\ell_{\max}$  follows from substituting  $\nu = -\tilde{\sigma}^2/2$ .

Note that  $\tilde{\sigma}$  as defined in (26) depends on the horizon  $t$ ; for the calibrated parameters it varies by less than 2% over  $t \in [30, 180]$  days, so we treat it as approximately constant.

*Proof.* Under the GBM approximation,  $\ln(\hat{Z}_t/\hat{Z}_0)$  is a Brownian motion with drift  $\nu = \tilde{\mu} - \tilde{\sigma}^2/2 = -\tilde{\sigma}^2/2$  and diffusion  $\tilde{\sigma}$ . The first-passage-time probability for a drifted Brownian motion to a fixed barrier is a classical result based on the reflection principle [Karatzas and Shreve, 1991], yielding (27) with drift parameter  $\nu$ .  $\square$

The moment-matching approximation captures the first two moments of  $Z_t$  but not higher-order properties such as skewness, and the first-passage-time formula (27) assumes a constant diffusion coefficient whereas  $\tilde{\sigma}$  in (26) is weakly  $t$ -dependent. Table 5 validates the approximation against Monte Carlo for the calibrated parameters, confirming errors below 0.2 pp for  $h \leq 0.70$ .

## 5.4 Constrained optimal hedge ratio

The liquidation probability (27) is increasing in  $h$  (since  $b$  decreases as  $h$  increases). Define

$$\bar{h}(\alpha) := \sup\{h \in [0, 1] : \Pr(\tau \leq T) \leq \alpha\}, \quad (28)$$

the maximum feasible hedge ratio for a given liquidation tolerance  $\alpha$ . The constrained optimal hedge ratio is then

$$h^{**} = \min(h^*, \bar{h}(\alpha)), \quad (29)$$

where  $h^*$  is the unconstrained optimum from Theorem 4.

**Remark 6.** *Under the calibration in Table 2, the unconstrained optimum is  $h^* = 0.977$  (Theorem 4), at which the liquidation probability exceeds 19% (Table 4). For any reasonable tolerance  $\alpha \leq 5\%$ , the constraint forces  $\bar{h}(\alpha) < h^*$ , yielding an interior solution  $h^{**} \approx 0.60$ – $0.65$  where the Sharpe ratio (inclusive of liquidation losses) is maximized.*

# 6 Monte Carlo Simulation

## 6.1 Calibration

We calibrate the model to on-chain data from a constant-product AMM pool and a lending protocol on the Sui blockchain. Token  $A$  is SUI and token  $B$  is NS (NaviSwap governance token). Volatilities and correlation are estimated from 91 days of daily CoinGecko price data using log-return standard deviations and the Pearson correlation of log returns.

Table 2: Baseline calibration parameters.

Parameter	Symbol	Value
Token <i>A</i> annualized volatility	$\sigma_A$	0.922
Token <i>B</i> annualized volatility	$\sigma_B$	1.084
Correlation	$\rho$	0.72
Token <i>A</i> borrow rate	$r_A$	0.03
Token <i>B</i> borrow rate	$r_B$	0.15
LP reward rate (farm + fees)	$R/V_0$	0.54
Stablecoin supply rate	$r_f$	0.04
Max LTV	$\ell_{\max}$	0.80
Collateral / LP ratio	$C/V_0$	2.0
Horizon	$T$	0.25 yr (90 days)

The LP reward rate of 54% includes both farm incentives ( $\approx 48\%$ ) and trading fees ( $\approx 6\%$ ) observed on the pool at the time of calibration. The asymmetry in borrow rates ( $r_B \gg r_A$ ) reflects the lower liquidity and higher demand for borrowing token *B*.

These reward rates reflect the token emission incentives commonly used by DeFi protocols to attract liquidity during their growth phase. Unlike yields in traditional finance, which are bounded by the risk-free rate and credit spreads, DeFi farming rewards are funded by protocol-native token emissions and can exceed 50% APR for early-stage pools. However, such rates tend to decline over time as total value locked (TVL) increases and emission schedules taper. To ensure that our conclusions are not contingent on elevated reward rates, Table 6 reports the optimal hedge ratio across a wide range of reward rates ( $R/V_0$  from 10% to 100%). The key finding—that the optimal hedge ratio lies in the range  $h^{**} \in [0.50, 0.70]$ —is robust for  $R/V_0 \geq 30\%$ , and the strategy remains viable (positive Sharpe ratio) for  $R/V_0 \geq 20\%$ .

## 6.2 Simulation design

We simulate  $N = 30,000$  paths of the correlated GBM pair  $(S_t^A, S_t^B)$  with daily time steps ( $\Delta t = 1/365$ ) over  $T = 90$  days. Correlated normal increments are generated via the Cholesky decomposition  $Z_2 = \rho Z_1 + \sqrt{1 - \rho^2} Z'_2$ , where  $Z_1, Z'_2$  are independent standard normals.

For each path and each hedge ratio  $h \in \{0, 0.20, 0.40, 0.50, 0.60, 0.65, 0.70, 0.80, 1.0\}$ , we compute:

1. The daily LTV. If  $LTV_t \geq \ell_{\max}$  for any  $t$ , the path is flagged as liquidated and assigned a penalty loss of  $0.20 \times C$ . This figure aggregates the protocol liquidation bonus (typically 5–10% of the repaid debt), market-impact slippage during forced selling, and the opportunity cost of the unwound position. On Sui-based protocols such as NAVI, the liquidation bonus is 5%; the 20% total accounts for adverse slippage in the thin markets characteristic of long-tail tokens.
2. LP rewards, claimed every 14 days and applied as partial debt repayment.
3. The terminal P&L  $\Pi_T - \Pi_0$  for surviving paths.

Let  $\bar{r}$  denote the sample mean ROE over the  $T$ -day period and  $\hat{\sigma}$  its sample standard deviation. The annualized Sharpe ratio is

$$\text{SR} = \frac{\bar{r} - r_f (T/365)}{\hat{\sigma}} \cdot \sqrt{\frac{365}{T}}, \quad (30)$$

where  $T$  is the horizon in days (here  $T = 90$ ; note that the analytical sections use  $T$  in years), scaling the per-period excess return and volatility to an annual basis.

## 7 Results

### 7.1 Optimal hedge ratio

Table 3 reports the simulation results across hedge ratios. The Sharpe ratio peaks at  $h \in [0.60, 0.65]$  (raw SR = 0.93–0.95), with  $h = 0.65$  marginally higher but  $h = 0.60$  within the flat region of the optimum.

Table 3: Monte Carlo results by hedge ratio ( $N = 30,000$  paths,  $T = 90$  days). “Raw” Sharpe excludes transaction costs; “+tx” includes a one-time 0.3% borrow fee and gas costs.

$h$ (%)	E[ROE]	Std	SR (raw)	SR (+tx)	P(loss)	P(liq)	5% VaR
0	+3.58	16.0	0.453	0.326	49.4%	0.0%	−15.4
20	+3.71	13.6	0.553	0.401	46.9%	0.0%	−12.6
40	+3.78	10.8	0.720	0.523	42.9%	0.1%	−9.2
50	+3.69	9.1	0.836	0.599	39.9%	0.4%	−7.5
<b>60</b>	<b>+3.32</b>	<b>7.4</b>	<b>0.931</b>	<b>0.636</b>	<b>36.0%</b>	<b>1.4%</b>	<b>−5.8</b>
<b>65</b>	<b>+3.06</b>	<b>6.7</b>	<b>0.951</b>	<b>0.622</b>	<b>32.6%</b>	<b>2.3%</b>	<b>−5.0</b>
70	+2.76	6.3	0.914	0.565	29.6%	3.4%	−4.2
80	+1.96	6.6	0.640	0.299	17.8%	7.0%	−19.3
100	−0.32	10.2	−0.030	−0.258	19.9%	19.2%	−21.2

E[ROE], Std, and VaR are in percentage points. E[ROE] and Std include transaction costs (matching the SR + tx column).

Figure 1 visualizes the trade-off: the Sharpe ratio peaks at  $h = 0.60$  and the liquidation probability rises sharply beyond  $h = 0.70$ .

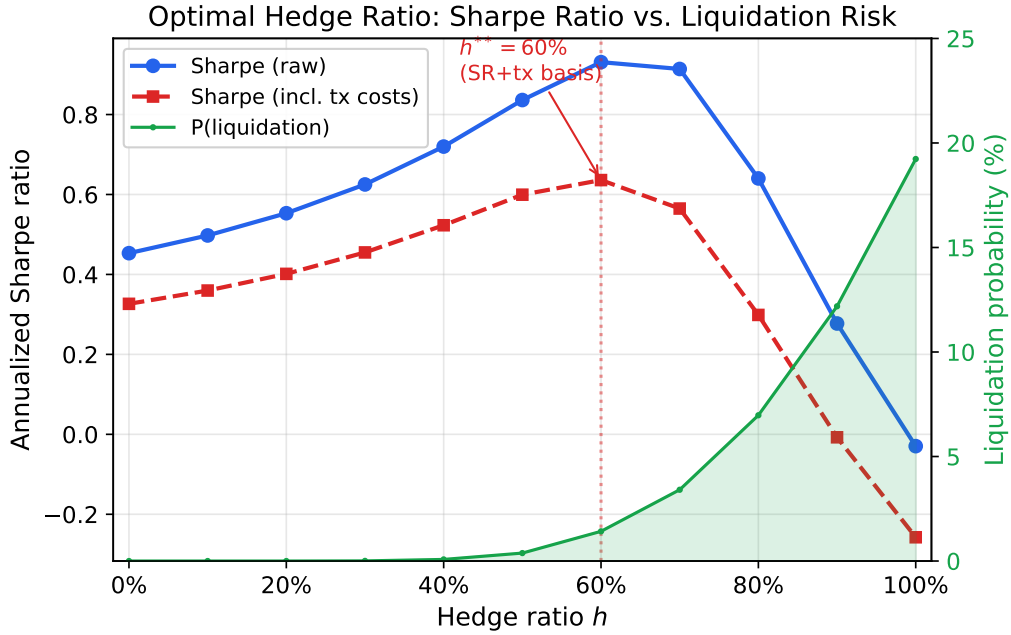


Figure 1: Sharpe ratio (left axis) and liquidation probability (right axis, green) as functions of the hedge ratio  $h$ . The optimal  $h^{**} = 60\%$  (on the SR + tx basis; raw SR is marginally higher at  $h = 0.65$ ) balances risk-adjusted return against liquidation risk.

Several patterns emerge:

- **Interior optimum.** The Sharpe ratio peaks in the range  $h = 0.60\text{--}0.65$  (raw:  $0.93\text{--}0.95$ ) and declines on both sides, confirming the analytical result.
- **Risk–return trade-off.** Increasing  $h$  from 0 to 0.60 reduces standard deviation from 16.0% to 7.4% while sacrificing only 0.26pp of expected return. Beyond  $h = 0.70$ , liquidation risk rises sharply (3.4% at  $h = 0.70$ , 19.2% at  $h = 1.0$ ), destroying risk-adjusted returns.
- **Transaction costs.** The one-time borrow fee (0.3% of borrowed amount) reduces the Sharpe ratio by 0.13–0.35 depending on hedge ratio, but does not shift the optimal  $h$ .

## 7.2 Liquidation analysis

Table 4 shows the liquidation statistics for the fully hedged case ( $h = 1.0$ , initial LTV = 50%).

Table 4: Liquidation statistics at  $h = 1.0$  ( $N = 30,000$ ,  $T = 90$  days).

Metric	No claims	Claim/14d
Liquidation probability	23.0%	19.2%
Mean max LTV	70.2%	67.8%
95th pctl max LTV	113.0%	108.2%
99th pctl max LTV	150.0%	144.5%

Regular reward claims reduce liquidation probability by  $\approx 4\text{pp}$ . Liquidated paths have an average price multiple of  $1.63\times$  (i.e., both tokens approximately doubled), while safe paths average  $0.82\times$ . This confirms that liquidation is driven by *rising* prices increasing debt value against fixed stablecoin collateral.

At the optimal  $h^{**} = 0.60$ , initial LTV drops to 30% and liquidation probability falls to 1.4%—well within the 5% tolerance assumed in Section 5.

**Accuracy of the analytical approximation.** Table 5 compares the first-passage-time approximation (27) with the Monte Carlo liquidation probability (without reward claims, to isolate the approximation error).

Table 5: Analytical (Eq. 27) vs. Monte Carlo liquidation probability ( $N = 50,000$  for tighter confidence intervals; main results use  $N = 30,000$ ).  $T = 90$  days, SUI/NS. MC(no) excludes reward claims; MC(cl) includes biweekly claims.

$h$ (%)	LTV <sub>0</sub>	$b$	Analytical	MC (no claims)	MC (claims)
30	15.0%	1.674	0.01%	0.01%	0.01%
40	20.0%	1.386	0.13%	0.12%	0.07%
50	25.0%	1.163	0.66%	0.66%	0.39%
60	30.0%	0.981	2.05%	2.02%	1.41%
70	35.0%	0.827	4.82%	4.65%	3.34%
80	40.0%	0.693	9.34%	8.97%	6.83%
100	50.0%	0.470	24.18%	22.88%	19.08%

The analytical approximation closely matches MC without reward claims (error  $< 0.2\text{pp}$  for  $h \leq 70\%$  and  $+1.3\text{pp}$  at  $h = 100\%$ ), validating the moment-matched GBM approximation of Section 5. The approximation slightly *overestimates* liquidation probability, making it a conservative bound. The gap between MC(no) and MC(cl) quantifies the risk-reduction benefit of biweekly reward claims.

Figure 2 decomposes the return–risk trade-off, showing that expected return decreases slowly with  $h$  while standard deviation drops sharply up to  $h \approx 0.70$ .

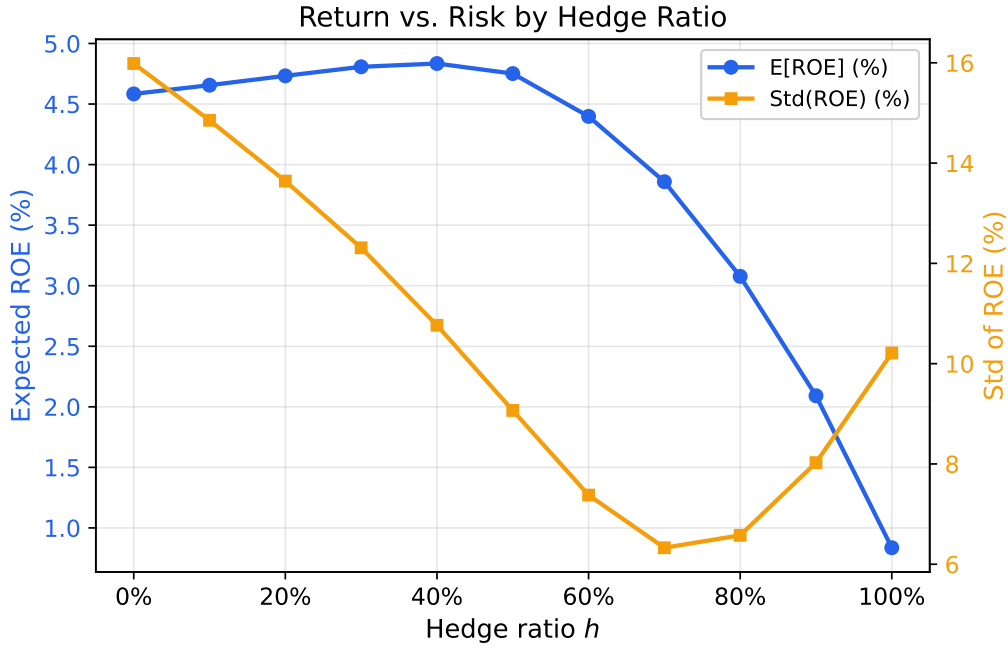


Figure 2: Expected ROE (left axis) and standard deviation of ROE (right axis) as functions of the hedge ratio. The variance reduction from hedging is substantial up to  $h \approx 0.70$ , after which liquidation losses cause both return and risk to deteriorate.

### 7.3 Sensitivity analysis

We examine how the optimal hedge ratio varies with the correlation  $\rho$  and the borrow rate  $r_B$ .

Figure 3 shows that the optimal  $h^{**}$  is robust to changes in correlation: across all tested values ( $\rho \in [0, 0.9]$ ), the Sharpe-maximizing hedge ratio remains in the range 60–70%. Higher correlation improves the overall Sharpe level (less price divergence) but does not materially shift the optimum.

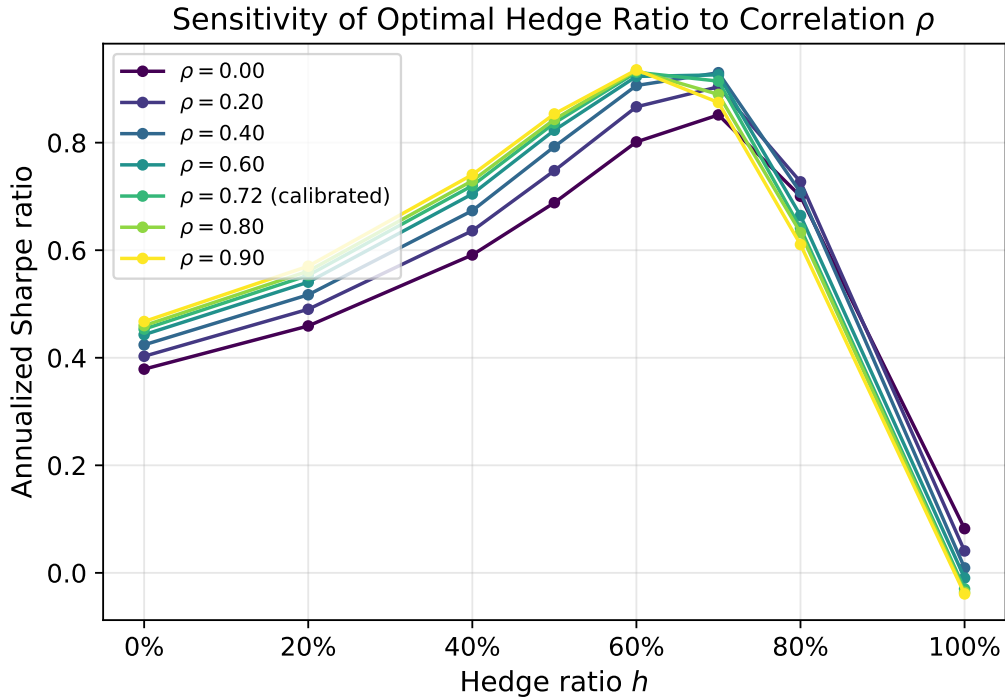


Figure 3: Sharpe ratio vs. hedge ratio for different correlation values  $\rho$ . The optimal  $h^{**}$  remains between 60% and 70% regardless of correlation.

Figure 4 shows sensitivity to the token  $B$  borrow rate. Higher borrow costs shift the optimal  $h^{**}$  slightly downward (from 70% at  $r_B = 5\%$  to 60% at  $r_B = 30\%$ ), consistent with Proposition 2: borrow cost is the only channel through which  $h$  affects expected return.

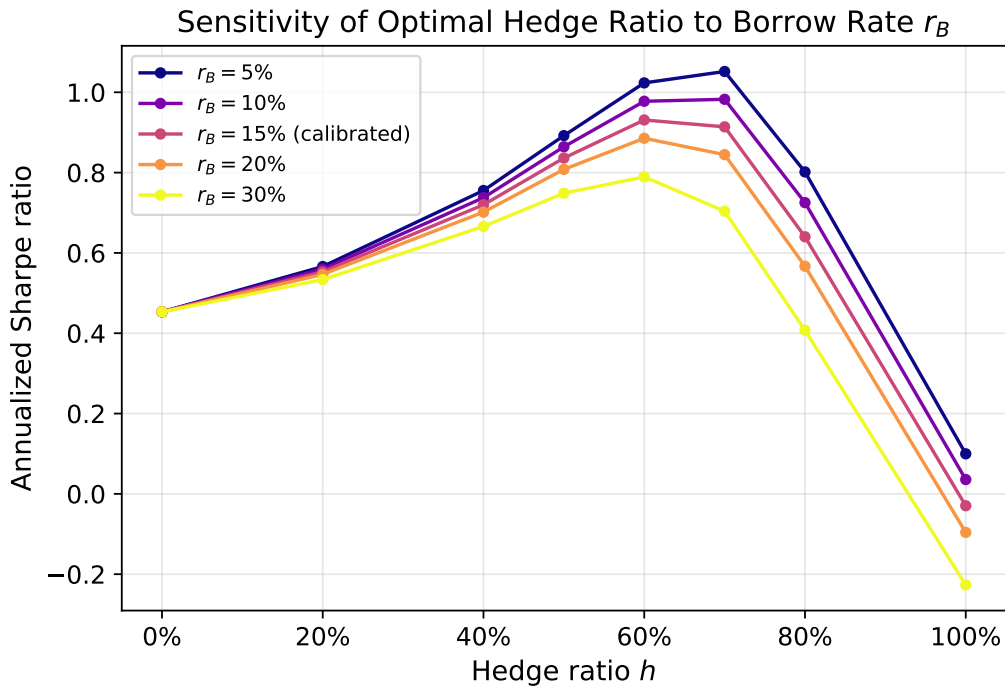


Figure 4: Sharpe ratio vs. hedge ratio for different borrow rates  $r_B$ . Higher borrow costs reduce overall Sharpe and shift the optimal hedge ratio slightly downward.

**Sensitivity to LP reward rate.** Table 6 shows how the optimal hedge ratio varies with the LP reward rate  $R/V_0$ . The reward rate is the primary driver of strategy viability: at  $R/V_0 = 10\%$ , the strategy is unprofitable at any hedge ratio, while at  $R/V_0 \geq 40\%$ , hedging becomes beneficial. The optimal hedge ratio increases with rewards (from  $h^{**} = 40\%$  at  $R/V_0 = 20\%$  to  $h^{**} = 70\%$  at  $R/V_0 = 70\%$ ), because higher rewards offset borrow costs and increase the margin for absorbing liquidation losses.

Table 6: Optimal hedge ratio by LP reward rate ( $N = 30,000$ ,  $T = 90$  days, SUI/NS parameters).

$R/V_0$	$h^{**}$	SR	Remark
10%	0%	-0.00	Strategy unprofitable
20%	40%	0.12	Marginal viability
30%	50%	0.30	
40%	60%	0.53	
54%	60%	0.93	Calibrated value
70%	70%	1.45	
100%	70%	2.41	

$h^{**}$  is evaluated on the grid of Table 3, which includes  $h = 0.65$ . At  $R/V_0 = 54\%$ , the raw Sharpe ratio peaks at  $h = 0.65$  (SR = 0.95); the transaction-cost-adjusted Sharpe peaks at  $h = 0.60$  (Table 3). Table 7 reports  $h^{**} = 65\%$  for SUI/NS on a finer 5% grid, consistent with the raw-SR ranking.

## 7.4 Robustness across token pairs

To verify that the optimal hedge ratio is not an artifact of the SUI/NS calibration, we replicate the Monte Carlo analysis for three additional token pairs on low-gas blockchains where delta-neutral LP strategies are practically viable. Table 7 reports the calibration parameters, estimated from 365 days of daily CoinGecko price data, together with representative lending and LP reward rates from each chain’s dominant protocols.

Table 7: Calibration parameters and optimal hedge ratios for additional token pairs ( $N = 30,000$ ,  $T = 90$  days,  $C/V_0 = 2.0$ , 5% hedge-ratio grid).

Pair	Chain	$\sigma_A$	$\sigma_B$	$\rho$	$r_A$	$r_B$	LP APR	$h^{**}$	SR
SUI/NS	Sui	92%	108%	0.72	3%	15%	54%	65%	0.95
SOL/RAY	Solana	80%	110%	0.83	5%	8%	40%	60%	0.68
SOL/JUP	Solana	80%	100%	0.86	5%	6%	35%	65%	0.67
ETH/ARB	Arbitrum	74%	103%	0.82	3%	5%	30%	60%	0.54

Using a fine 5% grid (rather than the coarser grid in Table 3), the Sharpe-maximizing hedge ratio falls in the range  $h^{**} \in [60\%, 65\%]$  across all four pairs—spanning three blockchains, correlations from 0.72 to 0.86, and annual volatilities from 74% to 110%. The absolute Sharpe ratio varies across pairs (0.54 for ETH/ARB to 0.95 for SUI/NS), reflecting differences in LP reward rates, but the optimal hedge ratio is tightly clustered. This confirms that the interior optimum arises from the *structural* interaction between hedging benefit and liquidation risk, not from pair-specific parameter values.

**Sensitivity to volatility level.** The baseline calibration uses a 91-day estimation window, and crypto-asset volatilities can shift substantially across regimes. Table 8 reports the optimal hedge ratio when both volatilities are scaled by  $\pm 20\%$ .

Table 8: Sensitivity to volatility level ( $N = 30,000$ ,  $T = 90$  days, all other parameters at baseline).

$\sigma$ scaling	$\sigma_A$	$\sigma_B$	$h^{**}$	SR	P(liq)
-20%	74%	87%	70%	1.64	1.1%
Baseline	92%	108%	65%	0.95	2.3%
+20%	111%	130%	50%	0.55	1.4%

The optimal hedge ratio shifts from 50% (high-vol regime) to 70% (low-vol regime), a 20 pp range centered on the baseline optimum. This is intuitive: lower volatility reduces the probability of large price moves that breach the LTV threshold, allowing higher hedge ratios. The finding reinforces the practical guideline to hedge conservatively (50–60%) during high-volatility periods and more aggressively (65–70%) during calm markets.

**Sensitivity to liquidation penalty.** The baseline simulation assumes a 20% collateral penalty upon liquidation. Since actual penalties vary across protocols (5–10% liquidation bonus plus variable slippage), Table 9 examines the impact of alternative penalty assumptions.

Table 9: Sensitivity to liquidation penalty ( $N = 30,000$ ,  $T = 90$  days, SUI/NS parameters).

Penalty	$h^{**}$	SR	P(liq) at $h^{**}$
10%	80%	1.18	7.0%
20%	65%	0.95	2.3%
30%	60%	0.85	1.4%

The optimal hedge ratio is sensitive to the liquidation penalty: at 10% penalty, the optimizer tolerates 7% liquidation probability and pushes  $h^{**}$  to 80%; at 30%, it retreats to 60% with only 1.4% liquidation probability. This confirms that the liquidation penalty is a key model input, and practitioners should calibrate it to their specific protocol’s liquidation bonus, typical slippage, and market depth.

## 7.5 Sensitivity to collateral ratio

The baseline analysis fixes  $C/V_0 = 2.0$ . Since the collateral ratio directly determines the liquidation buffer, we examine how  $h^{**}$  varies with  $C/V_0$ . Table 10 reports the optimal hedge ratio for  $C/V_0 \in [1.2, 5.0]$  using the SUI/NS calibration.

Table 10: Optimal hedge ratio and initial LTV as functions of the collateral ratio  $C/V_0$  ( $N = 30,000$ ,  $T = 90$  days, SUI/NS parameters).

$C/V_0$	$h^{**}$	SR	P(liq)	E[ROE]	Init LTV
1.2	30%	0.62	0.3%	+6.15%	25.0%
1.5	50%	0.71	2.3%	+4.64%	33.3%
1.8	60%	0.84	2.5%	+4.27%	33.3%
2.0	65%	0.95	2.3%	+4.16%	32.5%
2.5	80%	1.27	2.2%	+3.80%	32.0%
3.0	80%	1.68	0.7%	+3.74%	26.7%
4.0	90%	3.00	0.2%	+3.24%	22.5%
5.0	100%	3.97	0.1%	+2.83%	20.0%

Two patterns emerge. First,  $h^{**}$  increases monotonically with  $C/V_0$ : more collateral relaxes the liquidation constraint, allowing higher hedge ratios. At  $C/V_0 = 5.0$ , the constraint becomes non-binding and  $h^{**}$  approaches the unconstrained optimum  $h^* \approx 0.977$ . Second, the initial LTV at the optimum clusters around 25–33%, suggesting that **maintaining an initial LTV near 30%** is a natural anchor across collateral configurations.

However, a higher  $C/V_0$  also dilutes capital efficiency: E[ROE] declines from +6.15% at  $C/V_0 = 1.2$  to +2.83% at  $C/V_0 = 5.0$ , because a larger share of capital is locked in low-yielding stablecoin collateral. The elevated Sharpe ratios at high  $C/V_0$  reflect reduced variance rather than higher returns. In practice, LPs face a capital allocation trade-off between risk reduction and return, and the choice of  $C/V_0$  should reflect individual risk preferences and opportunity costs.

## 7.6 Rebalancing frequency

We compare five rebalancing strategies, all starting at  $h = 0.60$ , in Table 11. The “threshold” strategy rebalances when either token’s effective hedge ratio drifts more than the specified number of percentage points from the target.

Table 11: Rebalancing strategy comparison ( $h = 0.60$ ,  $N = 30,000$ ,  $T = 90$  days).

Strategy	E[ROE]	Std	SR	P(liq)	Avg rebal.	Cost
No rebalance	+4.41	7.15	0.965	1.4%	0.0	0%
Threshold 20pp	+4.98	7.25	1.108	1.3%	0.2	< 0.01%
Threshold 15pp	+5.14	7.28	1.148	1.3%	0.5	< 0.01%
Threshold 10pp	+5.26	7.32	1.178	1.2%	1.2	< 0.01%
Every 14 days	+5.30	7.32	1.186	1.2%	6.0	< 0.01%
Every 30 days	+5.36	7.34	1.198	1.2%	3.0	< 0.01%

E[ROE] and Std are in percentage points. E[ROE] here excludes the one-time entry/exit costs (borrow fee and gas) reported in Table 3; the difference of approximately 1.1 percentage points accounts for the apparent discrepancy between the two tables.

The key finding is that **any** rebalancing improves risk-adjusted returns over the static hedge. The threshold-based strategies achieve most of the benefit (Sharpe 1.15 at 15pp threshold) with far fewer trades than periodic rebalancing. Rebalancing costs are negligible on Sui (gas  $\approx$  \$0.01 per transaction).

A 15pp drift threshold represents a practically appealing rule: with the calibrated volatilities, the median time to trigger is approximately 62–85 days, meaning the LP rebalances roughly once per quarter.

## 7.7 Robustness to jump risk

The baseline model assumes geometric Brownian motion, which understates the frequency of large price moves observed in cryptocurrency markets. To assess whether the optimal hedge ratio is an artifact of the continuous-path assumption, we repeat the Monte Carlo analysis under a Merton jump-diffusion model [Merton, 1976].

Each token price follows

$$\frac{dS_t^i}{S_t^i} = (\mu_i - \lambda\kappa) dt + \sigma_i^d dW_t^i + J_i dN_t, \quad (31)$$

where  $N_t$  is a Poisson process with intensity  $\lambda$ ,  $J_i = e^{Z_i} - 1$  with  $Z_i \sim \mathcal{N}(\mu_J, \sigma_J^2)$  is the random jump size, and  $\kappa = \mathbb{E}[J_i] = e^{\mu_J + \sigma_J^2/2} - 1$  is the compensator ensuring  $\mathbb{E}[dS/S] = \mu_i dt$  in the absence of diffusion. Let  $N_t^c$ ,  $N_t^A$ ,  $N_t^B$  be independent Poisson processes with intensities  $\lambda\rho_J$ ,  $\lambda(1-\rho_J)$ ,  $\lambda(1-\rho_J)$  respectively. Token  $i$  experiences jumps from both  $N_t^c$  (common shocks affecting both tokens simultaneously) and  $N_t^i$  (idiosyncratic shocks); the total jump intensity per token is  $\lambda$ .

We calibrate the jump parameters to stylized facts of crypto markets:  $\lambda = 4$  jumps/year,  $\mu_J = -0.05$  (slight downward bias),  $\sigma_J = 0.15$ , and  $\rho_J = 0.80$  (high co-jump probability). The diffusion volatilities  $\sigma_i^d$  are reduced so that the *total* annualized variance matches the GBM calibration:  $(\sigma_i^d)^2 = \sigma_i^2 - \lambda(\mu_J^2 + \sigma_J^2)$ .

Table 12: GBM vs. Merton jump-diffusion ( $N = 30,000$ ,  $T = 90$  days, SUI/NS parameters). Jump parameters:  $\lambda = 4/\text{yr}$ ,  $\mu_J = -0.05$ ,  $\sigma_J = 0.15$ ,  $\rho_J = 0.80$ .

$h$ (%)	GBM			Jump-diffusion		
	SR	P(liq)	5% VaR	SR	P(liq)	5% VaR
0	0.45	0.0%	-14.4	0.45	0.0%	-14.5
40	0.72	0.1%	-8.2	0.72	0.1%	-8.2
60	0.93	1.4%	-4.7	0.93	1.5%	-4.8
<b>65</b>	<b>0.95</b>	<b>2.3%</b>	<b>-3.8</b>	<b>0.94</b>	<b>2.3%</b>	<b>-3.9</b>
70	0.91	3.4%	-3.1	0.93	3.3%	-3.1
100	-0.03	19.2%	-20.0	-0.01	18.9%	-20.0

VaR is in percentage points. All values exclude transaction costs; cf. Table 3 for tx-inclusive figures.

Table 12 shows that the optimal hedge ratio is unchanged at  $h^{**} = 65\%$  under variance-matched jump-diffusion with  $\rho_J = 0.80$ . The Sharpe ratio differs by less than 0.02 at every hedge ratio, and the liquidation probability changes by less than 0.2 pp.

A natural concern is that this robustness is an artifact of matching total variance. To address this, we run two additional stress tests: (i) reducing jump correlation to  $\rho_J = 0.30$  (predominantly idiosyncratic jumps), and (ii) leaving the diffusion volatility at the full GBM level so that jumps *add* to total variance rather than substituting for it. Table 13 reports the results at  $h = 65\%$  across all four combinations.

Table 13: Jump-diffusion stress tests at  $h = 65\%$  ( $N = 30,000$ ,  $T = 90$  days). “Matched” adjusts diffusion volatility so total variance equals GBM; “unmatched” keeps full GBM diffusion volatility, so jumps increase total variance.

$\rho_J$	Variance	SR	P(liq)	5% VaR	$h^{**}$
GBM (baseline)		0.95	2.3%	−3.8	65%
0.80	matched	0.94	2.3%	−3.9	65%
0.30	matched	0.94	2.1%	−3.9	65%
0.80	unmatched	0.83	2.8%	−4.4	65%
0.30	unmatched	0.81	2.7%	−4.4	65%

VaR is in percentage points.

The optimal hedge ratio  $h^{**} = 65\%$  is invariant across all four scenarios. When jumps add to total variance (unmatched rows), the Sharpe ratio drops from 0.95 to 0.81–0.83 and liquidation probability rises from 2.3% to 2.7–2.8%, but the *location* of the optimum does not shift. Reducing jump correlation from  $\rho_J = 0.80$  to 0.30 has negligible impact on  $h^{**}$ .

This robustness arises because the binding constraint is the *level* of initial LTV (30–33% at  $h = 0.60$ – $0.65$ ), which provides a large buffer that absorbs even idiosyncratic jumps. Nevertheless, if jumps are both large and purely idiosyncratic ( $\rho_J \rightarrow 0$ )—for instance, a token-specific short squeeze or protocol exploit—debt can spike without an offsetting increase in LP value, sharply raising liquidation risk. This asymmetric exposure remains the structural vulnerability of any delta-neutral strategy funded by collateralized borrowing; the 65% hedge ratio mitigates but cannot eliminate it.

## 8 Discussion

### 8.1 Practical guidelines

The results suggest the following guidelines for LPs operating delta-neutral strategies with collateralized borrowing:

- Hedge 50–70% of LP exposure.** Full hedging ( $h = 1$ ) is suboptimal due to elevated liquidation risk and borrow costs. A 60–65% hedge captures most of the variance reduction while maintaining a safe LTV buffer. (The raw Sharpe ratio is marginally maximized at  $h = 0.65$ , while the transaction-cost-adjusted Sharpe peaks at  $h = 0.60$ ; the difference is small and both lie within the flat optimum region.)
- Maintain collateral  $\geq 2 \times$  LP value.** This ensures the initial LTV at  $h = 0.60$  is  $\approx 30\%$ , providing ample margin before the 80% liquidation threshold.
- Rebalance when hedge drift exceeds 15pp.** This threshold-based rule balances performance improvement against transaction frequency.
- Claim and repay biweekly.** Regular reward claims reduce outstanding debt and lower liquidation risk by  $\approx 4\text{pp}$ .

5. **Monitor for correlated price surges.** Liquidation is triggered by *rising* prices (which increase debt value), not falling prices. Both tokens rising 60%+ simultaneously is the primary danger scenario.

## 8.2 Limitations

Several modeling assumptions warrant discussion:

- **GBM dynamics.** Cryptocurrency prices exhibit heavier tails and jumps than GBM. Section 7.7 shows that a Merton jump-diffusion model with matched total variance leaves the optimal hedge ratio and liquidation probabilities essentially unchanged, but regime-switching dynamics with persistent volatility shifts remain untested.
- **Constant rates.** Borrow and reward rates are assumed fixed, but in practice they fluctuate with market conditions. In particular, reward rates decline as pool TVL increases (dilution effect). Table 6 shows that the strategy is sensitive to the reward rate: at  $R/V_0 < 20\%$ , the strategy becomes unviable regardless of hedge ratio.
- **Static analytical framework.** The first-passage-time bound  $\bar{h}(\alpha)$  assumes a static hedge held over  $[0, T]$ . The rebalancing analysis (Table 11) shows that dynamic adjustment improves Sharpe ratios, implying that the analytical bound is conservative when rebalancing is employed.
- **No concentrated liquidity.** We consider only full-range constant-product pools. Concentrated liquidity (e.g., Uniswap v3) amplifies both IL and fee income, potentially shifting the optimal  $h$ .
- **Simplified liquidation.** We model liquidation as a fixed 20% collateral penalty (Section 6), whereas actual DeFi protocols implement partial liquidation (typically 50% of debt per event), liquidation bonuses (5–10%), and keeper response lags. The aggregate penalty is conservative for high-liquidity pairs but may understate losses for thin markets.
- **Price-taker assumption.** The model assumes that the LP’s position is small relative to the pool and lending market. Large positions may move borrow rates, dilute LP rewards, or impact pool prices, limiting the strategy’s capacity.

## 8.3 Extensions

Natural extensions of this work include:

- Generalization to concentrated-liquidity AMMs, where the LP value function  $V_t^{\text{LP}}$  is piecewise and depends on the tick range.
- Incorporation of stochastic borrow and reward rates, potentially modeled as mean-reverting processes correlated with token prices. In particular, utilization-dependent borrow rates—where short-squeeze dynamics during bull markets can cause rate spikes—would capture an important real-world risk channel.
- Multi-asset pools with more than two tokens, requiring vector-valued hedge ratios.

- Empirical validation using historical on-chain data from multiple pools across different blockchains.
- Joint optimization of the collateral ratio  $C/V_0$  and hedge ratio  $h$ , incorporating capital opportunity costs and alternative risk criteria such as the Kelly criterion.

## 9 Conclusion

We have studied the problem of optimally hedging the price exposure of liquidity positions in constant-product AMMs when the hedge is implemented through collateralized borrowing. The key insight is that the hedge ratio is not a binary choice (hedge or not) but a continuous variable whose optimum reflects a three-way trade-off:

1. **Variance reduction:** higher  $h$  reduces the portfolio’s exposure to divergent price movements (price divergence risk).
2. **Borrow cost:** higher  $h$  incurs more borrowing expense, linearly reducing expected return.
3. **Liquidation risk:** higher  $h$  raises the loan-to-value ratio, increasing the probability of forced liquidation.

We showed that the unconstrained Sharpe ratio is maximized at  $h^* \approx 0.977$ —near-full hedging—under typical DeFi parameters (Corollary 5), but at this hedge ratio the liquidation probability exceeds 19%. The practical interior optimum  $h^{**} \approx 0.60$  therefore arises from the binding liquidation constraint—the central finding of this paper. The liquidation probability was bounded using a first-passage-time approximation (Proposition 6), yielding a maximum feasible hedge ratio  $\bar{h}(\alpha)$  that determines the constrained optimum  $h^{**} = \min(h^*, \bar{h}(\alpha))$ .

Monte Carlo simulations calibrated to on-chain data from a SUI/NS pool confirmed the analytical results: the optimal hedge ratio is  $h^{**} \approx 0.60$ – $0.65$ , achieving a Sharpe ratio of 0.93–0.95 (raw) with a liquidation probability of only 1.4–2.3%. The first-passage-time approximation was validated against Monte Carlo, showing errors below 0.2pp in the relevant range (Table 5). This result is robust: replication across three additional token pairs (SOL/RAY, SOL/JUP, ETH/ARB) spanning three blockchains, with correlations from 0.72 to 0.86 and volatilities from 74% to 110%, yields  $h^{**} \in [60\%, 65\%]$  under  $C/V_0 = 2.0$ . Threshold-based rebalancing (15pp drift) further improves the Sharpe ratio to 1.15 with minimal transaction costs.

These results provide actionable guidance for DeFi liquidity providers: partial hedging (50–70%) dominates both the unhedged and fully hedged extremes, and a simple rebalancing rule maintains the hedge without excessive trading. The analytical framework generalizes to any constant-product pool with collateralized borrowing available for the constituent tokens.

## References

Adams, H., Zinsmeister, N., Salem, M., Keefer, R., and Robinson, D. Uniswap v2 Core. Technical report, Uniswap, 2020.

- Aigner, A. A. and Dhaliwal, G. UNISWAP: Impermanent Loss and Risk Profile of a Liquidity Provider. *arXiv preprint arXiv:2106.14404*, 2021.
- Angeris, G., Kao, H.-T., Chiang, R., Noyes, C., and Chitra, T. An Analysis of Uniswap Markets. In *Cryptoeconomic Systems*, 2020.
- Bartoletti, M., Chiang, J. H., and Lafuente, A. L. SoK: Lending Pools in Decentralized Finance. In *Financial Cryptography*, 2021.
- Capponi, A. and Jia, R. The Adoption of Blockchain-based Decentralized Exchanges. *arXiv preprint arXiv:2103.08842*, 2021.
- Clark, J. The Replicating Portfolio of a Constant Product Market. *SSRN preprint*, 2020.
- Evans, A., Angeris, G., and Chitra, T. Optimal Fees for Geometric Mean Market Makers. In *ACM DeFi*, 2022.
- Fan, Y., Francisco, N., and Pinter, J. Differential Liquidity Provision in Uniswap v3 and Implications for Contract Design. *arXiv preprint arXiv:2204.00716*, 2022.
- Gudgeon, L., Perez, D., Harz, D., Livshits, B., and Gervais, A. The Decentralized Financial Crisis. In *Crypto Valley Conference on Blockchain Technology*, 2020.
- Heimbach, L., Wang, Y., and Wattenhofer, R. Risks and Returns of Uniswap V3 Liquidity Providers. In *ACM AFT*, 2022.
- Karatzas, I. and Shreve, S. E. *Brownian Motion and Stochastic Calculus*. Springer, 2nd edition, 1991.
- Khakhar, A. and Chen, X. Delta Hedging Liquidity Positions on Automated Market Makers. *arXiv preprint arXiv:2208.03318*, 2022.
- Lipton, A., Lucic, V., and Sepp, A. Unified Approach for Hedging Impermanent Loss of Liquidity Provision. *Digital Finance*, 2025.
- Loesch, S., Hindman, N., Richardson, M. B., and Welch, N. Impermanent Loss in Uniswap v3. *arXiv preprint arXiv:2111.09192*, 2021.
- Merton, R. C. Option Pricing When Underlying Stock Returns Are Discontinuous. *Journal of Financial Economics*, 3(1–2):125–144, 1976.
- Milevsky, M. A. Asian Options, the Sum of Lognormals, and the Reciprocal Gamma Distribution. *Journal of Financial and Quantitative Analysis*, 33(3):409–422, 1998.
- Milionis, J., Moallemi, C. C., Roughgarden, T., and Zhang, A. L. Automated Market Making and Loss-Versus-Rebalancing. *arXiv preprint arXiv:2208.06046*, 2022.
- Perez, D., Werner, S. M., Xu, J., and Livshits, B. Liquidations: DeFi on a Knife-edge. In *Financial Cryptography*, 2021.
- Pintail. Uniswap: A Good Deal for Liquidity Providers? Medium, 2019.
- Qin, K., Zhou, L., and Gervais, A. Quantifying Blockchain Extractable Value: How Dark is the Forest? In *IEEE S&P*, 2022.

## A Derivation of Variance Components

We provide full derivations of the variance components  $v_{GG}$ ,  $v_{AA}$ , and  $v_{GA}$  from Section 4.4.

**Notation.** Let  $p_A = e^{X_T}$ ,  $p_B = e^{Y_T}$ ,  $G = \sqrt{p_A p_B} = e^{(X_T + Y_T)/2}$ , and  $A = \frac{1}{2}(p_A + p_B)$ . All expectations are under zero-drift GBM ( $\mu_A = \mu_B = 0$ ).

$$v_{GG} = \text{Var}(G).$$

$$\begin{aligned} \mathbb{E}[G^2] &= \mathbb{E}[p_A p_B] = e^{\rho\sigma_A\sigma_B T} && \text{(Lemma 1, } a = b = 1) \\ (\mathbb{E}[G])^2 &= e^{-2\phi T} && \text{(Table 1)} \\ v_{GG} &= e^{\rho\sigma_A\sigma_B T} - e^{-2\phi T}. \end{aligned}$$

$$v_{AA} = \text{Var}(A).$$

$$\begin{aligned} \text{Var}(p_A) &= \mathbb{E}[p_A^2] - (\mathbb{E}[p_A])^2 = e^{\sigma_A^2 T} - 1, \\ \text{Var}(p_B) &= e^{\sigma_B^2 T} - 1, \\ \text{Cov}(p_A, p_B) &= \mathbb{E}[p_A p_B] - \mathbb{E}[p_A]\mathbb{E}[p_B] = e^{\rho\sigma_A\sigma_B T} - 1, \\ v_{AA} &= \text{Var}\left(\frac{p_A + p_B}{2}\right) = \frac{1}{4}[\text{Var}(p_A) + \text{Var}(p_B) + 2\text{Cov}(p_A, p_B)] \\ &= \frac{1}{4}[e^{\sigma_A^2 T} + e^{\sigma_B^2 T} + 2e^{\rho\sigma_A\sigma_B T} - 4]. \end{aligned}$$

$$v_{GA} = \text{Cov}(G, A).$$

$$\begin{aligned} \text{Cov}(G, A) &= \frac{1}{2}[\text{Cov}(G, p_A) + \text{Cov}(G, p_B)], \\ \text{Cov}(G, p_A) &= \mathbb{E}[G p_A] - \mathbb{E}[G]\mathbb{E}[p_A] = \mathbb{E}[p_A^{3/2} p_B^{1/2}] - e^{-\phi T}, \\ \mathbb{E}[p_A^{3/2} p_B^{1/2}] &= e^{(3\sigma_A^2 - \sigma_B^2 + 6\rho\sigma_A\sigma_B)T/8} \quad (a = \frac{3}{2}, b = \frac{1}{2}), \\ \text{Cov}(G, p_B) &= \mathbb{E}[p_A^{1/2} p_B^{3/2}] - e^{-\phi T}, \\ \mathbb{E}[p_A^{1/2} p_B^{3/2}] &= e^{(-\sigma_A^2 + 3\sigma_B^2 + 6\rho\sigma_A\sigma_B)T/8}, \\ v_{GA} &= \frac{1}{2}[e^{(3\sigma_A^2 - \sigma_B^2 + 6\rho\sigma_A\sigma_B)T/8} + e^{(-\sigma_A^2 + 3\sigma_B^2 + 6\rho\sigma_A\sigma_B)T/8} - 2e^{-\phi T}]. \end{aligned}$$

## B Derivation of the Sharpe FOC

The Sharpe ratio is  $\text{SR}(h) = \mu(h)/\sigma(h)$  where  $\mu(h) = \mu_0 - ch$  (linear) and  $\sigma^2(h) = V_0^2(v_{GG} + h^2 v_{AA} - 2h v_{GA})$  (quadratic).

**First-order condition.** Setting  $\text{SR}'(h) = 0$ :

$$\begin{aligned} \frac{d}{dh} \frac{\mu}{\sigma} &= \frac{\mu' \sigma - \mu \sigma'}{\sigma^2} = 0 \\ \Rightarrow \mu' \sigma^2 &= \mu \cdot \sigma \sigma' = \mu \cdot \frac{1}{2} (\sigma^2)'. \end{aligned}$$

Substituting  $\mu' = -c$  and  $(\sigma^2)' = V_0^2(2hv_{AA} - 2v_{GA})$ , and canceling  $V_0^2$ :

$$-c(v_{GG} + h^2 v_{AA} - 2hv_{GA}) = (\mu_0 - ch)(hv_{AA} - v_{GA}). \quad (32)$$

Expanding the left-hand side:

$$\text{LHS} = -cv_{GG} - ch^2 v_{AA} + 2chv_{GA}.$$

Expanding the right-hand side:

$$\text{RHS} = \mu_0 hv_{AA} - \mu_0 v_{GA} - ch^2 v_{AA} + chv_{GA}.$$

The  $-ch^2 v_{AA}$  terms cancel on both sides, leaving:

$$-cv_{GG} + 2chv_{GA} = \mu_0 hv_{AA} - \mu_0 v_{GA} + chv_{GA}.$$

Collecting  $h$ -terms on the right and constants on the left:

$$\mu_0 v_{GA} - cv_{GG} = h(\mu_0 v_{AA} - cv_{GA}).$$

This is linear in  $h$ , yielding the unique solution

$$h^* = \frac{\mu_0 v_{GA} - cv_{GG}}{\mu_0 v_{AA} - cv_{GA}}.$$

**Second-order condition.** Define  $f(h) := \text{SR}^2(h) = \mu^2(h)/\sigma^2(h)$ . Since  $\text{SR}$  and  $f$  share the same critical points (for  $\mu > 0$ ), it suffices to verify  $f''(h^*) < 0$ . We have

$$f'(h) = \frac{2\mu\mu'\sigma^2 - \mu^2(\sigma^2)'}{\sigma^4},$$

and at  $h^*$  where  $\mu'\sigma^2 = \mu \cdot \frac{1}{2}(\sigma^2)'$ ,

$$f''(h^*) = \frac{2(\mu')^2\sigma^2(h^*) - \mu(h^*)^2(\sigma^2)''(h^*)}{\sigma^4(h^*)}.$$

Since  $(\sigma^2)'' = 2V_0^2 v_{AA} > 0$ , the numerator equals  $2c^2\sigma^2(h^*) - \mu(h^*)^2 \cdot 2V_0^2 v_{AA}$ . The first term is positive and the second is negative. For  $\mu_0 \gg c$  (which holds in practice), the second term dominates and  $f''(h^*) < 0$ , confirming that  $h^*$  is a maximum.

**Numerical verification.** Under the calibration in Table 2:  $h^* = (0.1369 \times 0.2376 - 0.0225 \times 0.2331) / (0.1369 \times 0.2431 - 0.0225 \times 0.2376) = 0.02729 / 0.02794 = 0.977$ , consistent with  $h_{\text{mv}} = v_{GA}/v_{AA} = 0.2376/0.2431 = 0.977$ .